NASA TECHNICAL NOTE

NASA TN D-1688

NASA TN D-1688

THE EFFECTIVENESS OF THREE EXIT VANE CASCADE CONFIGURATIONS FOR VECTORING THE THRUST OF A DUCTED FAN

by Kenneth W. Mort and Paul F. Yaggy

Ames Research Center
Moffett Field, Calif.

NATIONAL AERONAUTICS AND SPACE ADMINISTRATION • WASHINGTON, D. C. • OCTOBER 1964

THE EFFECTIVENESS OF THREE EXIT VANE CASCADE CONFIGURATIONS FOR VECTORING THE THRUST OF A DUCTED FAN

By Kenneth W. Mort and Paul F. Yaggy

Ames Research Center
Moffett Field, Calif.

NATIONAL AERONAUTICS AND SPACE ADMINISTRATION

For sale by the Office of Technical Services, Department of Commerce,
Washington, D.C. 20230 -- Price $0.75

THE EFFECTIVENESS OF THREE EXIT VANE CASCADE CONFIGURATIONS FOR VECTORING THE THRUST OF A DUCTED FAN

By Kenneth W. Mort and Paul F. Yaggy

Ames Research Center
Moffett Field, Calif.

SUMMARY

The thrust vectoring effectiveness was evaluated for three vane configurations by examining the aerodynamic characteristics obtained with vane deflection angles from 0° to 100°, fan advance ratios from 0 to just under 0.7, and at duct angles of attack from 0° to 90°.

Analysis of the results indicated that it would be undesirable to use vanes of the type tested to produce large amounts of thrust vectoring because of the magnitude of the accompanying losses in performance. However, the vanes did have the capability of producing small amounts of thrust vectoring and large pitching-moment changes without significant losses in performance. Because of this, the vanes are potentially an efficient source of longitudinal trim and control for ducted fan powered vehicles.

INTRODUCTION

A 4-foot-diameter ducted fan mounted on a wing tip had been tested previously to obtain aerodynamic data for a wide range of operating conditions including those corresponding to VTOL transitions from hover to forward flight and return. In these tests, the thrust of the ducted fan was vectored to produce direct lift at hover and low speed by tilting the duct relative to the airstream at angles from 0° to 90°. The results of these tests were presented in reference 1.

It is apparent that the thrust of a ducted fan can be vectored by means other than or in conjunction with tilting the duct. Results of tests with a single vane in the duct exit (ref. 2) suggested the desirability of using exit vanes for this purpose. To provide data for estimating the practicality and limitations of this concept, tests were made of three different exit vane arrangements using the same ducted fan as used in the tests reported in reference 1. Aerodynamic data were obtained for a wide range of advance ratios and duct angles of attack for vane deflection angles from 0° to 100°. The results of these tests are presented herein.

NOTATION

b	fan blade chord, in.
c	exit vane chord, ft
c_d	original duct chord, ft
C_D	drag coefficient, $\frac{\text{drag}}{qd_e c_d}$
C_L	lift coefficient, $\frac{L}{qd_e c_d}$
C_m	pitching-moment coefficient, $\frac{M}{qd_e c_d^2}$
C_P	power coefficient, $\frac{P}{\rho n^3 d^5}$
C_{l_i}	blade-section design lift coefficient, $\frac{12(\text{section design lift})}{qb}$
d	fan diameter, ft
d_e	duct exit diameter, ft
g	gap between exit vanes, ft
h	fan blade thickness, in.
J	fan advance ratio, $\frac{V}{nd}$
L	lift, lb
M	pitching moment, ft-lb
n	fan rotational speeds, rps
P	power, ft-lb/sec
P_o	power without cascade, ft-lb/sec
q	free-stream dynamic pressure, lb/ft^2
r	radial distance from duct center line, ft
R	fan radius, ft
T_o	thrust without cascade, lb
V	free-stream velocity, ft/sec

X longitudinal force, positive upstream, lb

α duct angle of attack, deg

β fan blade angle measured at tip (unless otherwise noted), deg

δ_c deflection of vane center section, referred to duct axis (fig. 3(b))

δ_n deflection of vane nose flap, referred to duct axis (fig. 3(b))

δ_v vane deflection referred to duct axis (fig. 3(b))

θ effective turning angle, $\tan^{-1}\frac{L}{X}$, deg

ρ mass density of air, slugs/ft^3

MODEL AND APPARATUS

General Characteristics

The ducted fan and semispan wing panel upon which the duct was mounted were the same as those of reference 1. The general arrangement of the ducted fan and wing mounted in the wind tunnel for testing is shown in figure 1. Ducted fan and wing dimensions and characteristics are presented in figure 2 and in tables I and II.

Exit Vane Cascades

The model was tested with three cascade configurations referred to hereafter as the 45° cascade with a vane chord-to-gap ratio of 1.66, the 0° cascade with a vane chord-to-gap ratio of 1.66, and the 0° cascade with a vane chord-to-gap ratio of 0.83. Figures 1(a) and (b) show the ducted fan with the first two configurations mounted in the wind tunnel and figure 3(a) shows the dimensions. The third configuration was the same as the second except that every other vane was removed, leaving only three vanes. The vanes removed are shown with dashed lines in figure 3(a).

The same vane design was used for all three configurations. Since it was desired to produce large turning angles efficiently, simulation of vanes with large amounts of camber was necessary. This was accomplished by designing the vanes with hinged leading- and trailing-edge flaps. Figure 3(b) shows the vane detail. Because of the necessity for large vane deflections and the accompanying clearance requirements, some of the vanes did not extend all the way to the shroud as can be seen from figures 1(a), 1(b), and 3(a). This, of course, had an adverse effect on the performance.

Instrumentation

Forces and moments on the ducted fan were measured independently of the wing and support structure by strain gages on the duct-trunnion support tube.

The power input to the motor which drove the ducted fan was recorded on a polyphase watt-meter. These readings were corrected for motor efficiency.

TESTS

The tests were conducted by setting an exit vane deflection and then varying the duct angle of attack at various advance ratios which ranged from 0 to about 0.7. For these advance ratios the free-stream dynamic pressure ranged from 0 to 34 psf and the fan rotational speed from 2300 to 4000 rpm. For the duration of the test, the wing, which served only as a fairing, was set at 0° angle of attack. The fan blade angle was set at a constant value of 15° measured at the tip.

REDUCTION OF DATA

Duct-Trunnion Strain-Gage Data

It was necessary to correct the indicated normal force and pitching moment to account for the torque reactions in the fan drive gear box. The torque reactions were computed from the power input data and were subtracted from the values indicated by the strain gages. The indicated thrust required no corrections.

Accuracy of Measuring Devices

The various measuring devices used were accurate within the following limits. These values include error limits involved in reading and reducing the data as well as the accuracy of the device itself.

Duct angle	$\pm 0.2^{\circ}$
Vane deflection angles	$\pm 0.5^{\circ}$
Lift	± 10 lb
Drag	± 10 lb
Pitching moment	± 30 ft-lb

Fan rotational speed	±0.5 rps
Shaft horsepower	±20 horsepower
Free-stream dynamic pressure	±0.2 lb/sq ft

RESULTS AND DISCUSSION

The data are presented in two sections. The first contains the results for static conditions at zero free-stream velocity. These data are presented as ratios of the static thrust and power with the exit vanes to those without the exit vanes at the same fan rotational speed. For most of the vane deflections zero free-stream velocity characteristics were examined at several rotational speeds. (The duct alone data were obtained from ref. 1.) The second section contains the results for various free-stream velocities. In this section the data are presented in a more conventional coefficient form (based on free-stream dynamic pressure and a reference area) as a function of fan advance ratio.

Aerodynamic Characteristics at Zero Free-Stream Velocity

These characteristics are shown in figures 4 through 6 for the three vane configurations. The characteristics indicate that with the fan rotational speed held constant, the addition of the undeflected vanes caused an increase in the resultant of the longitudinal and lift forces of all three configurations. For the 45° cascade this resultant force decreased continuously with vane deflection up to the maximum tested vane deflection of 100° where the effective turning angle produced was about 80°. For the 0° cascade with vane chord-to-gap ratio of 1.66, little or no reduction in resultant force occurred at vane deflections up to 40° where the effective turning angle was about 30°; however, greater deflections produced large reductions in resultant force. Test data were obtained for the 0° cascade with the 0.83 vane chord-to-gap ratio for vane deflections only up to 50° where the effective turning angle produced was about 18°. At this deflection there appeared to be a slight increase in resultant force. It would be anticipated that somewhat larger vane deflections would produce losses in resultant force similar to those shown for the other 0° cascade.

The power variations of figures 4 through 6 indicate that for all three configurations the presence of the undeflected vanes resulted in an increase in the power required. The power required decreased slightly with vane deflection for the 45° cascade but increased markedly for both 0° configurations.

The static performance of the duct with the three different vane configurations at various effective turning angles was compared with that for the duct without vanes. This was done by computing a figure of merit for

each vane configuration based on the resultant force vector and the exit area of the duct without vanes installed. The figure of merit for the duct alone is given in reference 1. The results of the comparison presented in figure 7 show that the presence of the undeflected vanes did not alter the figure of merit even though both the thrust and power were increased. This was not anticipated for the 0° cascade because vanes which greatly reduce exit area should reduce the figure of merit.

It is also apparent from figure 7 that, as the vanes are deflected the figure-of-merit ratio decreases; however, up to about 20° of effective turning, the loss is less than 10 percent. At larger values of effective turning the efficiency of the duct with vanes is substantially lower than that for the tilting duct without vanes.[1]

The results of reference 3 showed that for a ducted fan with exit vanes, tested over a range of disc loadings from 130 to 290 psf, there were no appreciable variations in vane turning effectiveness with disc loading. Similarly, no variation was noted for the ducted fan of this investigation for the range of disc loadings from 35 to 90 psf. The large amount of scatter in the data shown in figures 4 through 6 occurred at the lower disc loadings where the measurement error was a relatively large percentage of the measured values. There was no systematic variation with disc loading in the data scatter.

Aerodynamic Characteristics at Free-Stream Velocities Other Than Zero

Figures 8, 9, and 10 show the aerodynamic characteristics in conventional coefficient form of the three vane configurations at several fan advance ratios and vane deflections. The required power corresponding to these conditions is shown in figure 11. The power data indicated that, for the range of duct angles tested, the power required for a given advance ratio and vane deflection was independent of the duct angle.[2] Hence, the power data are presented for zero duct angle of attack only.

It is obvious from the results presented in figures 8, 9, and 10 that a given lift increment can be produced by rotating the duct or by deflecting the vanes or by a combination of both. However, to produce large lift increments deflecting the vanes caused larger increases in drag as well as larger changes in trim than tilting the duct. Smaller lift increments, however, can be produced by vane deflection without undue losses in performance, but the trim changes are still rather large.

---

[1]The 0° cascade with the 0.83 chord-to-gap ratio was not tested beyond effective turning angles of 19° (50° vane deflection), but its efficiency would probably be somewhat less than that of the 0° cascade with the 1.66 chord-to-gap ratio at effective turning angles greater than 20°.

[2]If for some of the test conditions the duct angle had been increased further, the power required probably would have increased.

Analysis of Results

Cascaded exit vanes in ducted fans have been proposed for VTOL applications to achieve the thrust vectoring necessary for transition and hovering flight. Proposals have included using only the exit vanes for thrust vectoring or using a combination of exit vanes and duct tilting. The results presented herein and those of reference 1 indicate that it would be more efficient to use duct tilting rather than either exit vanes alone or in combination with duct tilting to obtain the large flow turning angles required for vertical take-off and landing. However, the capability of the exit vanes to produce large pitching moment changes and small amounts of thrust vectoring without significant loss in performance does have practical advantage, as indicated in the following two applications.

In references 2 and 4, it was indicated that a single exit vane could be used to provide longitudinal trim independent of forward velocity for the flight range from hover to forward flight. This was done without significantly increasing the power required. The present investigation has shown that if greater pitching-moment control power is necessary it can be obtained with cascaded vanes with no significant losses in performance.

In reference 1, it was noted that operation of the duct at high duct angles of attack and low power input often produced stalling of the upstream duct lip which was accompanied by large changes in pitching moment and performance. Since operating conditions of this nature may be encountered during low power descents, a limitation in the rate of descent allowable is indicated. Such a boundary was determined for the airplane described in references 2 and 4, which used this same duct. This boundary was presented in figure 11(b) of reference 1 and is reproduced in figure 12 of this report. A reduction in the duct angle required at a constant power would have the effect of delaying the lip stall to a higher rate of descent. The ability of the exit vanes to produce small amounts of flow turning without significant increases in power required would accomplish this purpose. An indication of the increase in allowable descent velocity before lip stall which might be achieved by this method is given in figure 12 for two vane settings of the 0° cascade with vane chord-to-gap ratio of 0.83.[3] For example, at 30 knots horizontal velocity, the allowable rate of descent could be increased from 400 to 1100 feet per minute by using a vane deflection of 50°.

Ames Research Center
National Aeronautics and Space Administration
Moffett Field, Calif., July 17, 1964

[3]It was assumed that the stall boundary defined in reference 1 would be the same for the ducted fan with or without the exit vanes. This assumption was substantiated by a few tests.

REFERENCES

1. Mort, Kenneth W., and Yaggy, Paul F.: Aerodynamic Characteristics of a 4-Foot-Diameter Ducted Fan Mounted on the Tip of a Semispan Wing. NASA TN D-1301, 1962.

2. Yaggy, Paul F., and Mort, Kenneth W.: A Wind-Tunnel Investigation of a 4-Foot-Diameter Ducted Fan Mounted on the Tip of a Semispan Wing. NASA TN D-776, 1961.

3. Aoyagi, Kiyoshi, Hickey, David H., and deSavigny, Richard A.: Aerodynamic Characteristics of a Large-Scale Model With a High Disk-Loading Lifting Fan Mounted in the Fuselage. NASA TN D-775, 1961.

4. Yaggy, Paul F., and Goodson, Kenneth W.: Aerodynamics of a Tilting Ducted Fan Configuration. NASA TN D-785, 1961.

TABLE I.- BASIC DIMENSIONS OF DUCTED FAN AND WING

Duct	
Inside diameter	4 ft
Outside diameter	4 ft 10.5 in.
Chord	2 ft 9 in.
Exit diameter	4 ft 6.3 in.
Diffuser angle	11°
Inlet guide vanes	
Chord	3 in.
Number of vanes	7
Airfoil section	NACA 65A010
Position of vane c/4, percent of duct chord	14.5 percent
Twist	0°
Fan	
Plan-form curves	(see fig. 3)
Number of blades	8
Hub to tip diameter ratio	0.333
Position of hub center line, percent of duct chord	29.3 percent
Design static thrust disc loading	150 psf
Design static power disc loading	7.96 hp/ft^2
Blade angle control	fixed pitch
Blade angle at tip	15°
Approximate blade tip clearance	0.030 in.
Stators	
Position of stator c/4, percent of duct chord	49.4 percent
Twist, centerbody to tip	15°
Eight stators with 6-inch chord	
Airfoil	NACA 0008.4
Mean line	a = 0.4
Additional 9-inch chord stator which housed fan drive shaft	
Airfoil	NACA 0017
Mean line	a = 0.4
Wing	
Airfoil section	NACA 2418
Area	48 ft^2
Semispan	8 ft
Mean aerodynamic chord	6.09 ft
Taper ratio	0.675

TABLE II.- SHROUD AND CENTERBODY COORDINATES

Shroud coordinates tabulated in percent of shroud chord (33 in.)			Centerbody coordinates tabulated in percent of centerbody length (71.5 in.)	
Chordwise length	Outside radius	Inside radius	Length	Radius
0	81.5	81.5	0	0
.5	81.4	79.6	.5	2.07
.75	83.8	79.0	1.25	3.20
1.25	84.4	78.4	2.50	4.46
2.5	85.4	77.2	5.0	6.17
5.0	86.4	75.8	7.5	7.40
7.5	87.1	74.9	10	8.31
10	87.6	74.2	15	9.68
15	88.2	73.3	20	10.54
20	88.6	72.9	25	11.01
25	88.6	72.7	25.875[a]	11.06
30	88.6	72.7	30	11.19
35	88.6	72.7	32.57[b]	11.19
40	88.6	72.7	40	11.19
45	88.6	72.7	50	11.19
50	88.6	72.7	60	11.19
55	88.6	73.2	70	10.49
60	88.6	74.1	72.05[c]	10.14
65	88.0	75.1	80	7.97
70	87.4	76.1	83.20	6.77
75	86.8	77.1	90	4.03
80	85.9	78.1	95	2.01
85	85.2	79.1	100	0
90	84.3	80.1		
95	83.3	81.1		
100	82.2	82.0		

[a]Shroud leading-edge position.
[b]Inlet guide vane c/4 line position.
[c]Shroud trailing-edge position.

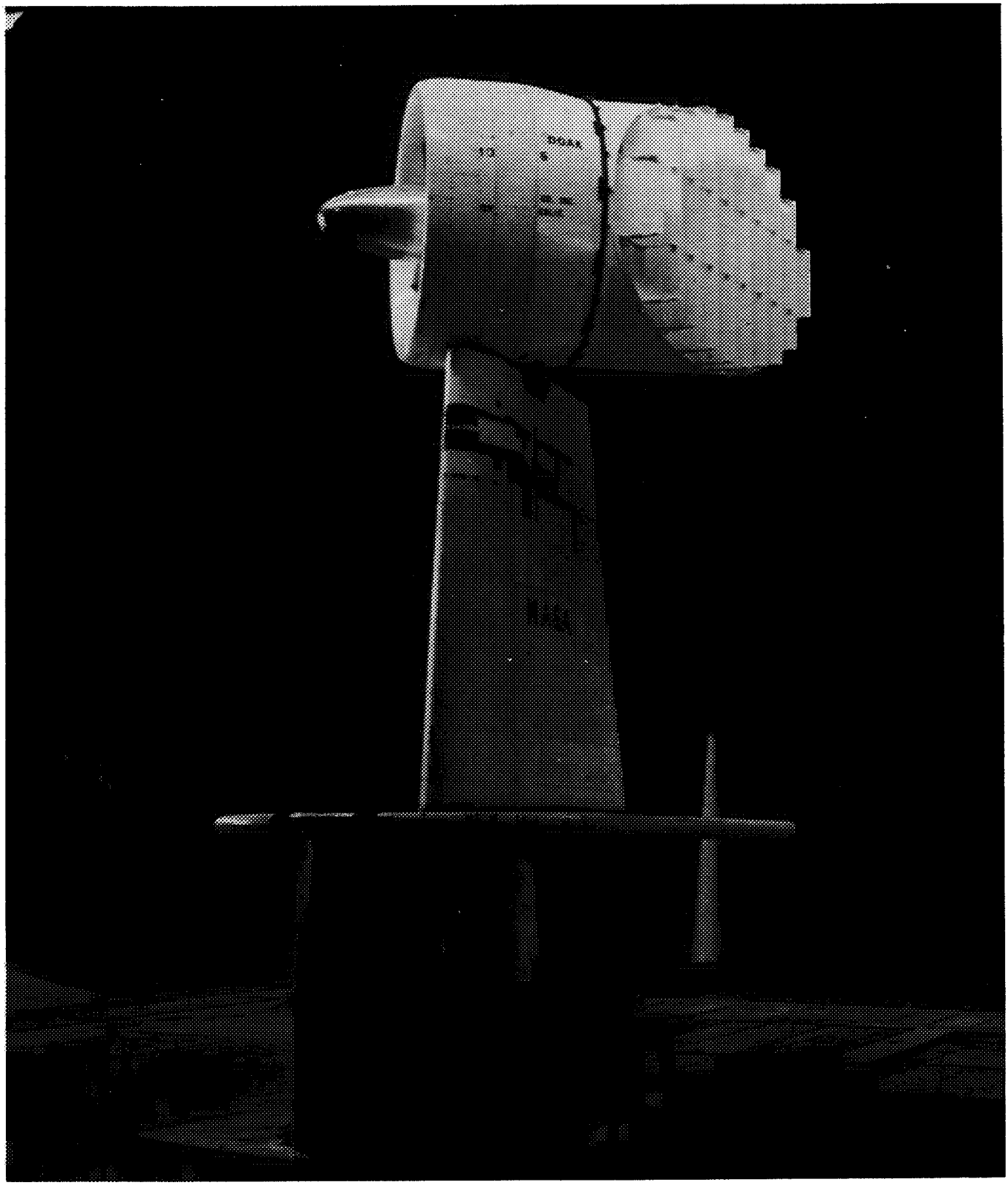

A-28982

(a) 45° cascade.

Figure 1.- Ducted fan model mounted in the Ames 40- by 80-Foot Wind Tunnel.

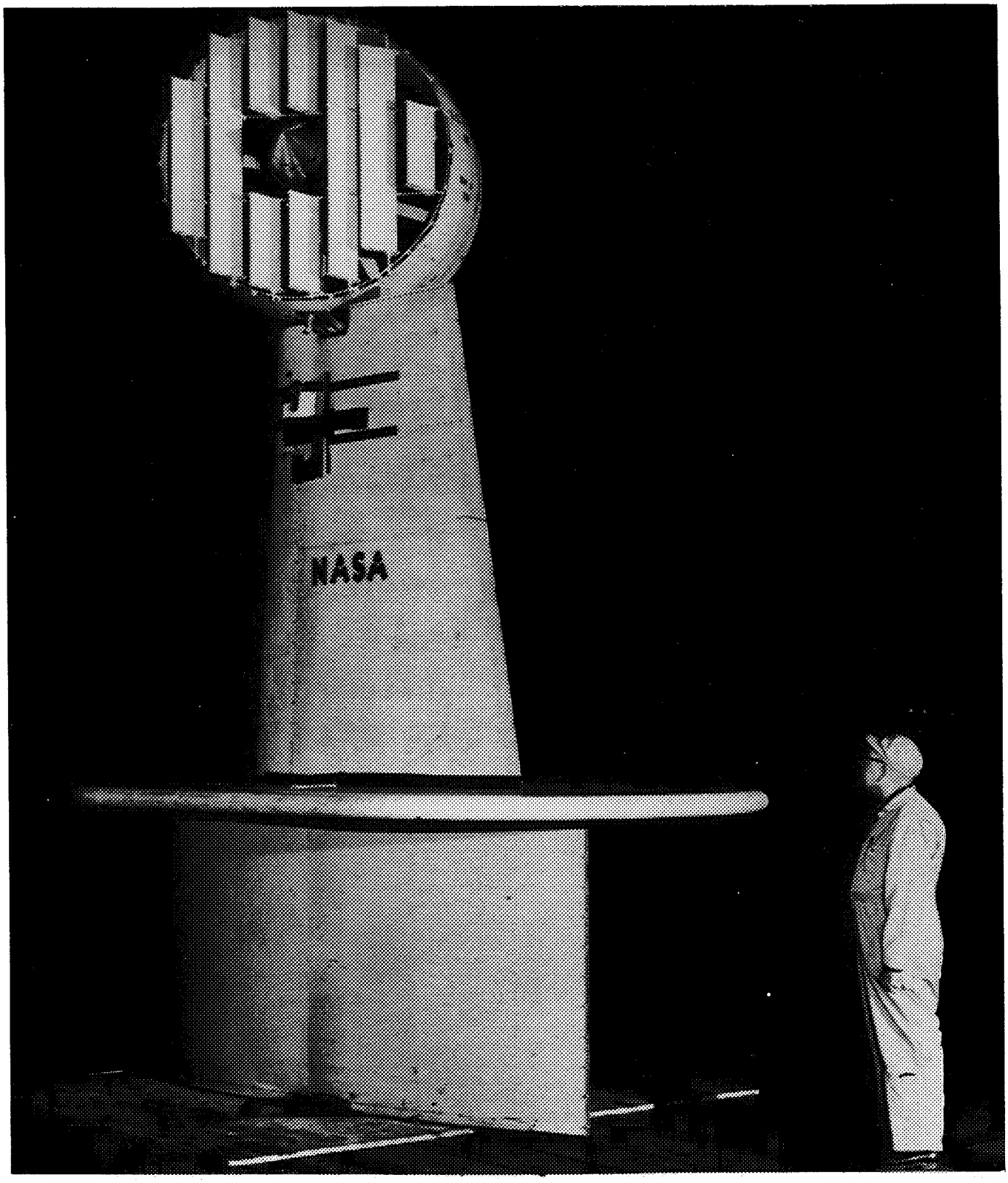

A-29016

(b) 0° cascade; c/g = 1.66.

Figure 1.- Concluded.

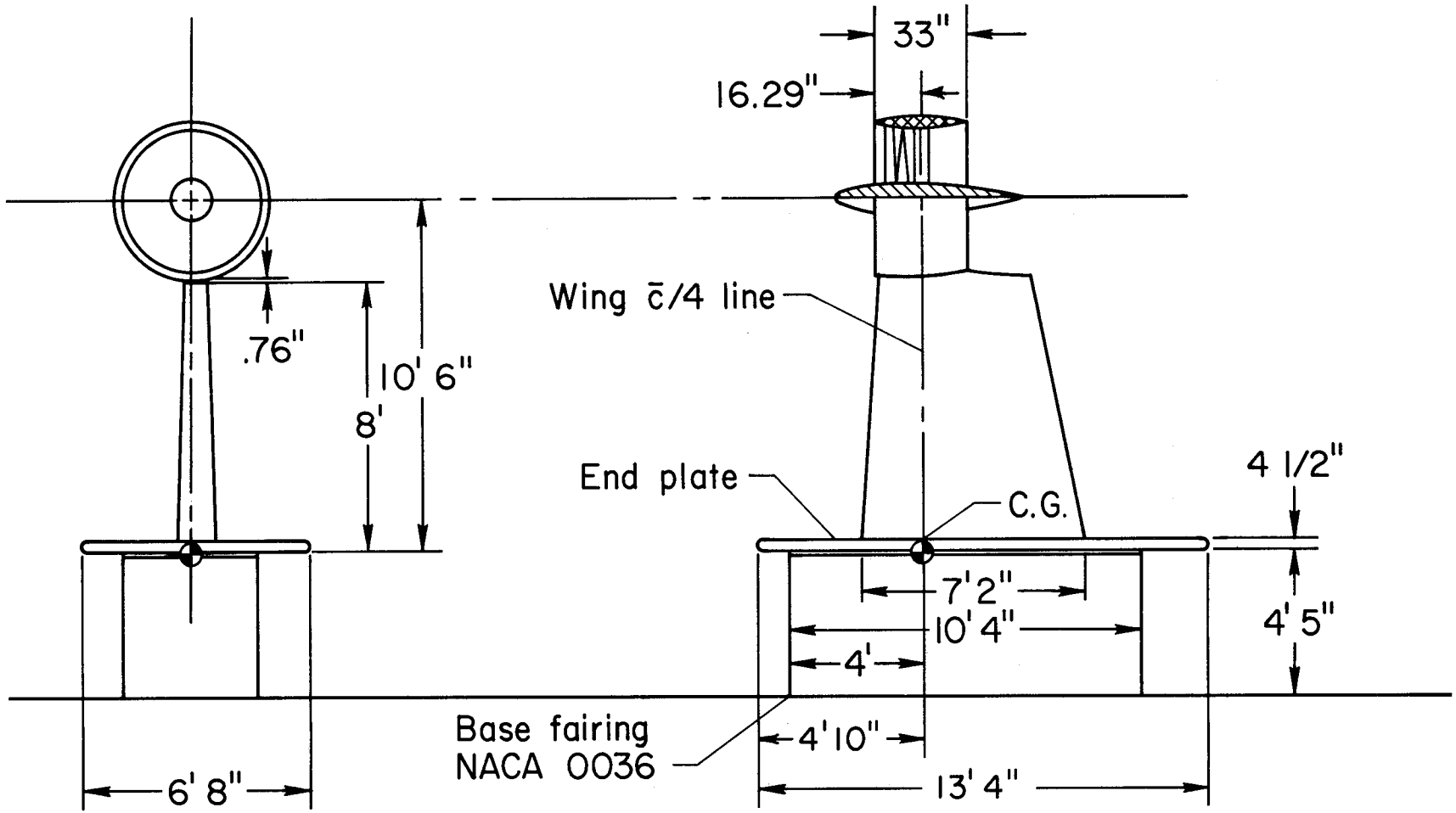

(a) Ducted fan and wing mounting details.

Figure 2.- Dimensions and characteristics of basic model.

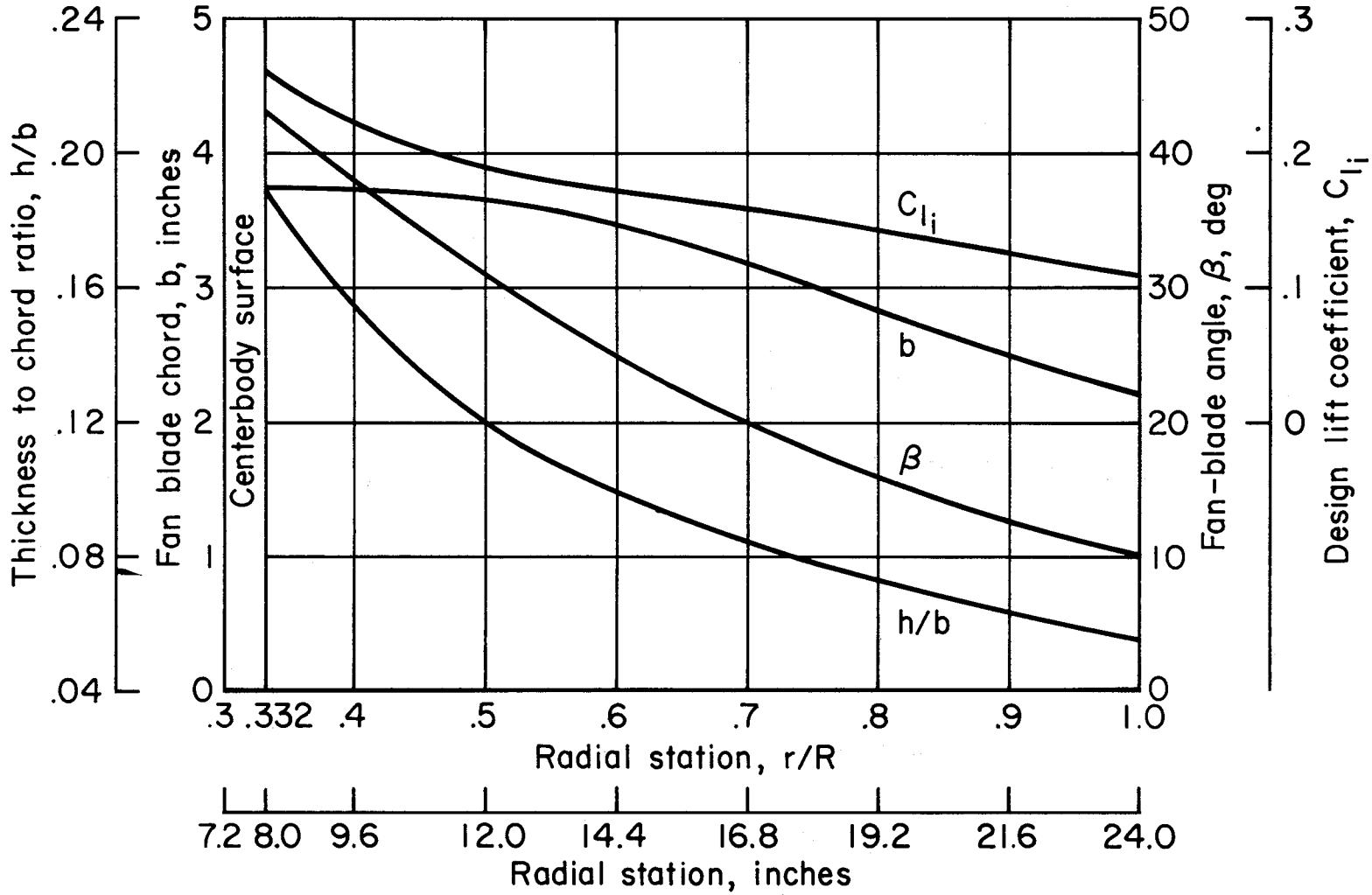

(b) Fan blade-form curves with the design lift coefficient, blade chord, blade angle, and blade thickness to chord ratio as functions of the radial distance from the duct center.

Figure 2.- Concluded.

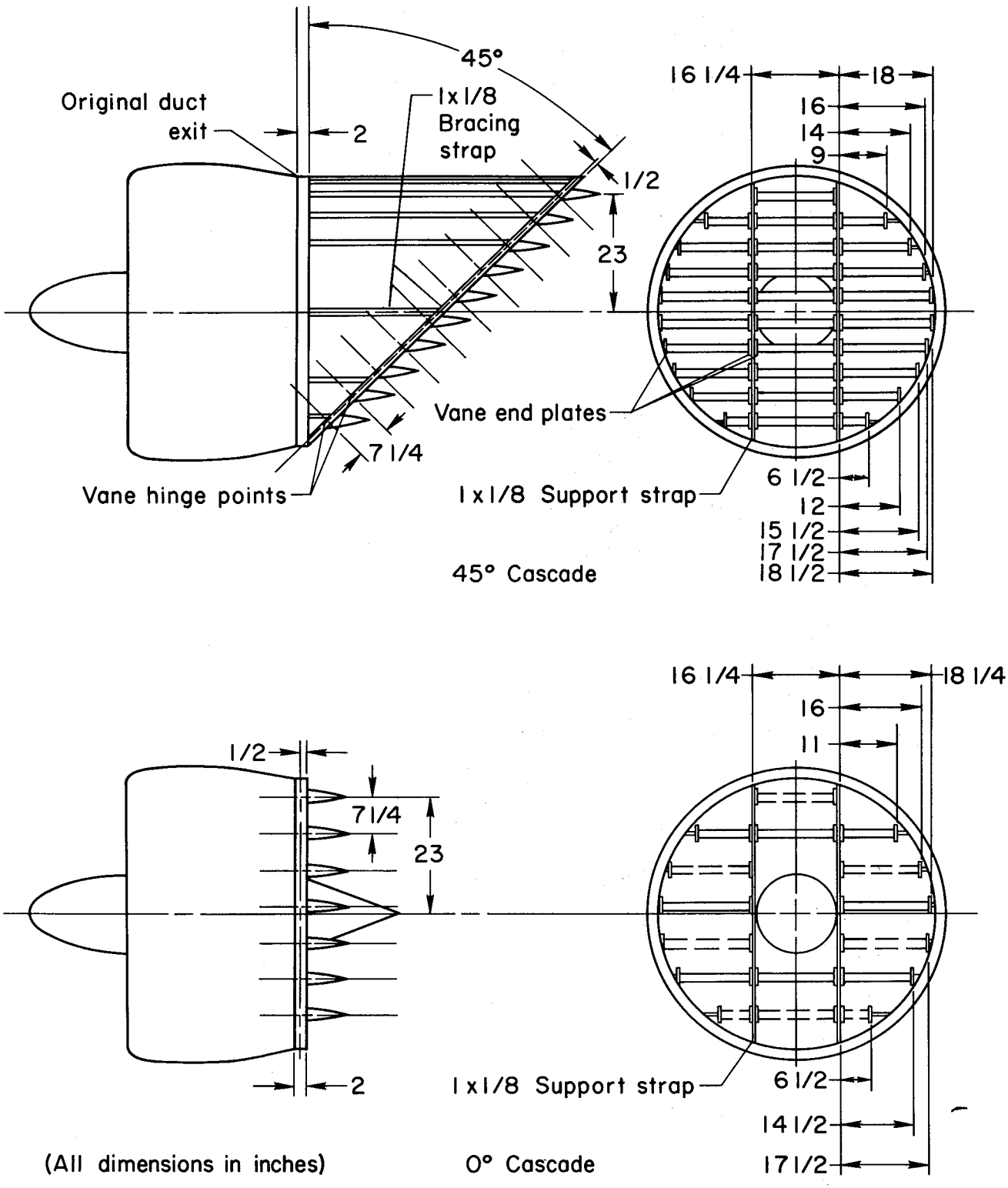

(a) Vane mounting detail.

Figure 3.- Exit vane dimensions and arrangement.

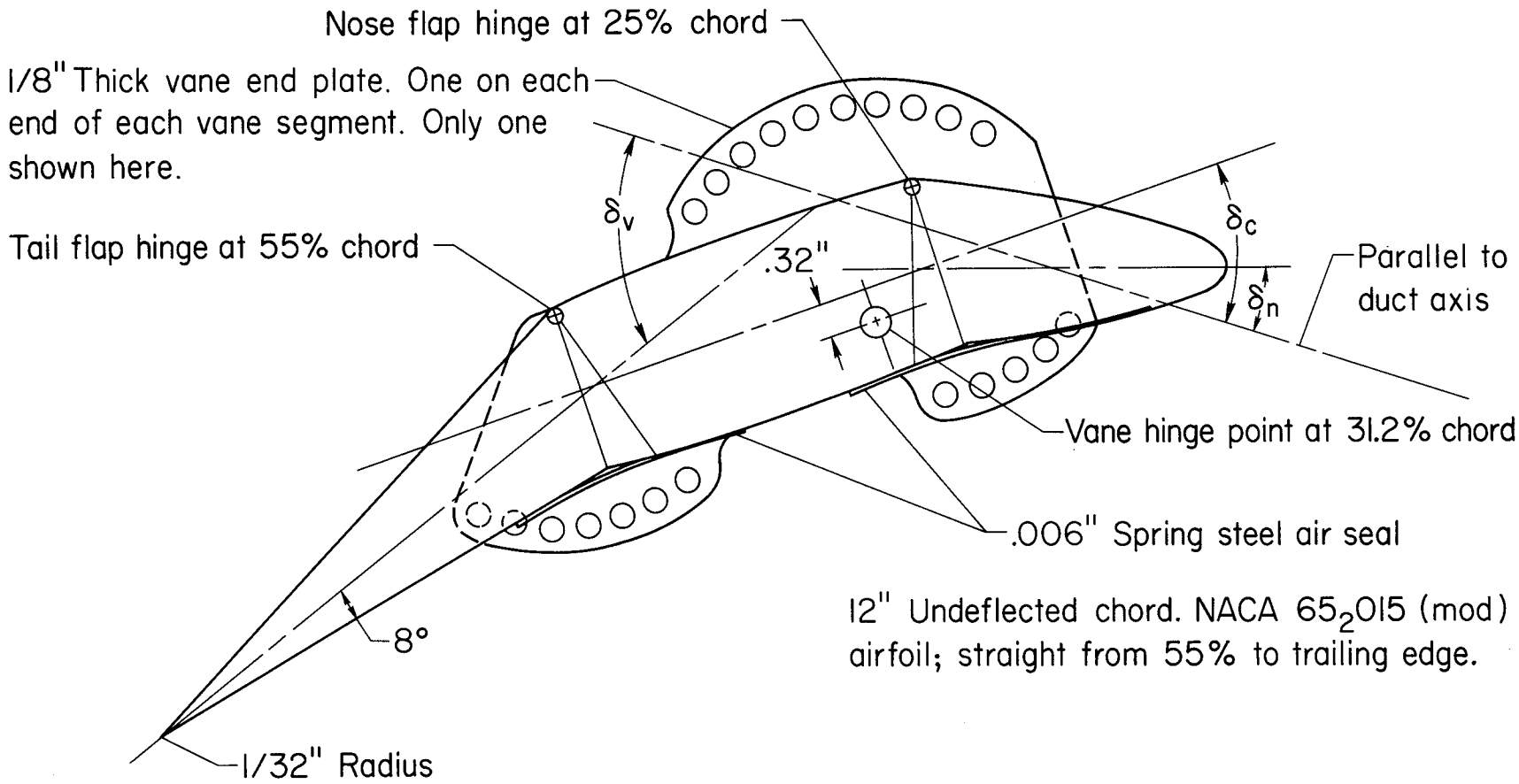

(b) Vane detail.

Figure 3.- Concluded.

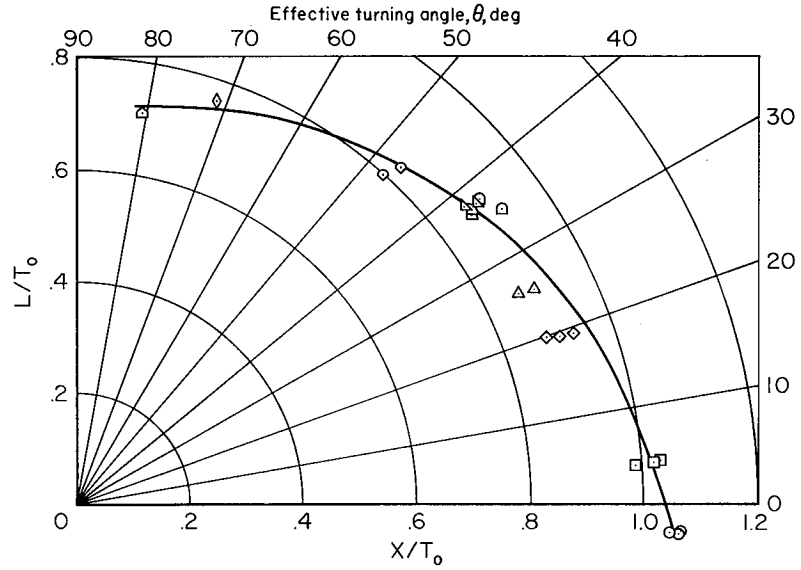

(a) Turning effectiveness.

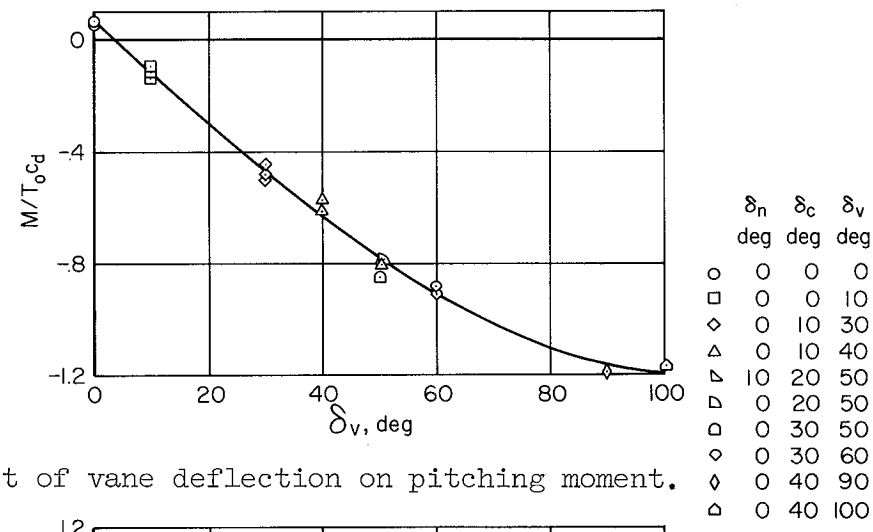

(b) Effect of vane deflection on pitching moment.

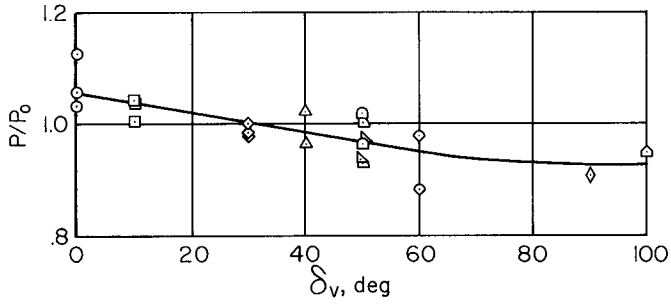

(c) Effect of vane deflection on power.

Figure 4.- Aerodynamic characteristics of the ducted fan with the 45° cascade with a vane chord-to-gap ratio of 1.66 at zero free-stream velocity; $\alpha = 0°$.

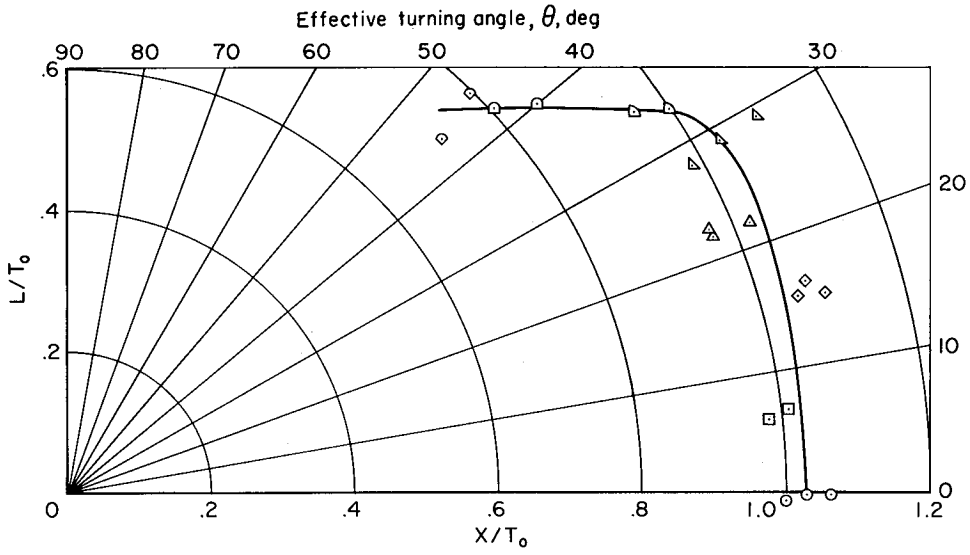

(a) Turning effectiveness.

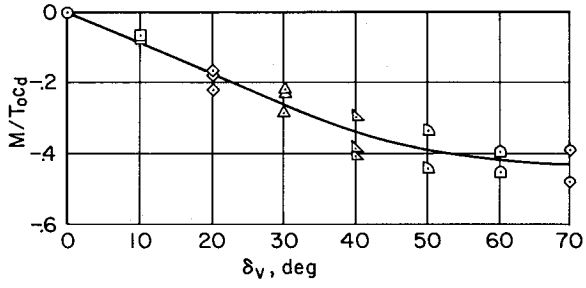

(b) Effect of vane deflection on pitching moment.

	δ_n deg	δ_c deg	δ_v deg
○	0	0	0
□	0	0	10
◇	0	20	20
△	0	10	30
◺	0	20	40
◻	0	20	50
◻	0	20	60
◇	0	20	70

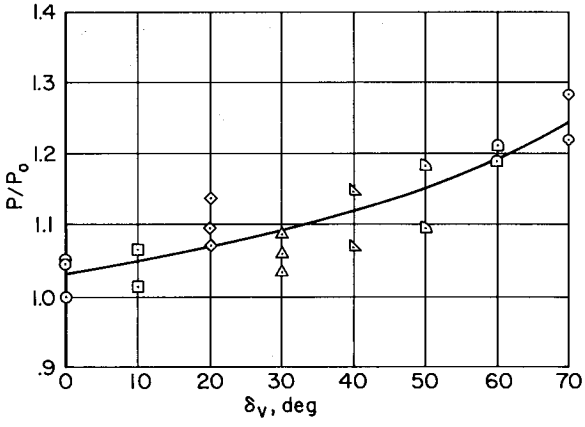

(c) Effect of vane deflection on power.

Figure 5.- Aerodynamic characteristics of the ducted fan with the 0° cascade with a vane chord-to-gap ratio of 1.66 at zero free-stream velocity; $\alpha = 0^\circ$.

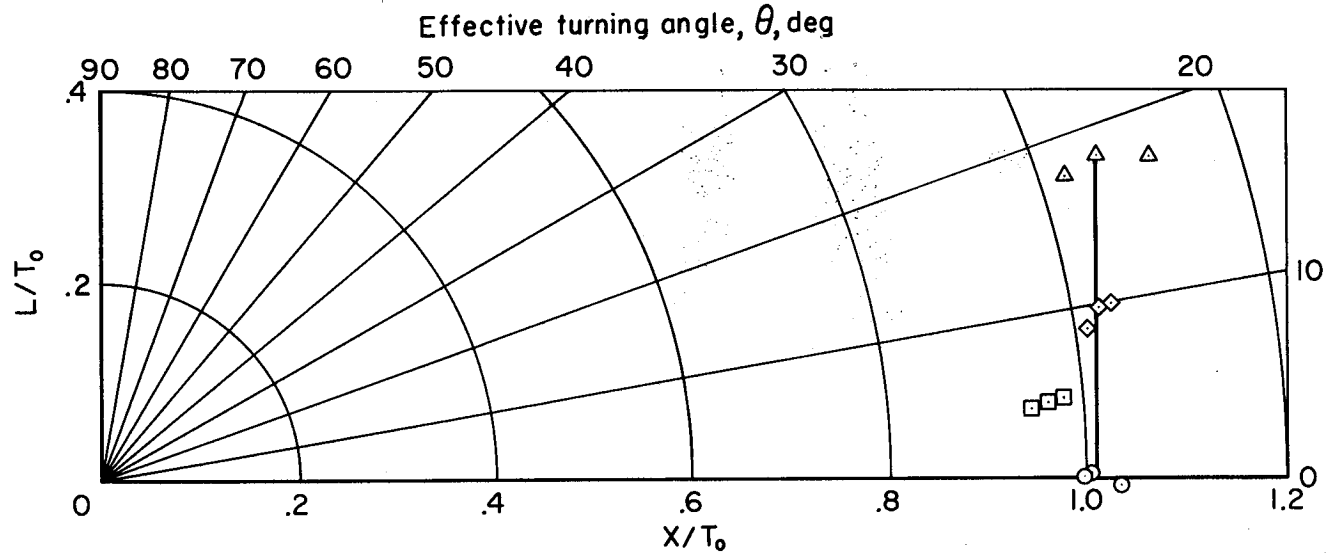

(a) Turning effectiveness.

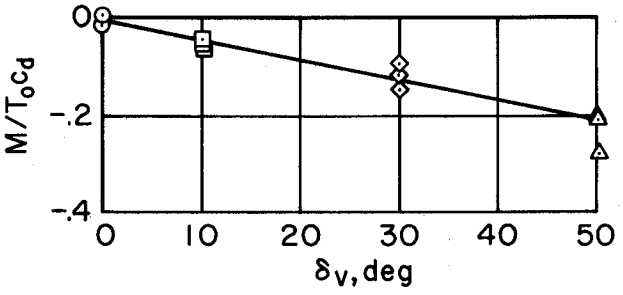

	δ_n deg	δ_c deg	δ_v deg
○	0	0	0
□	0	0	10
◇	0	0	30
△	10	10	50

(b) Effect of vane deflection on pitching moment.

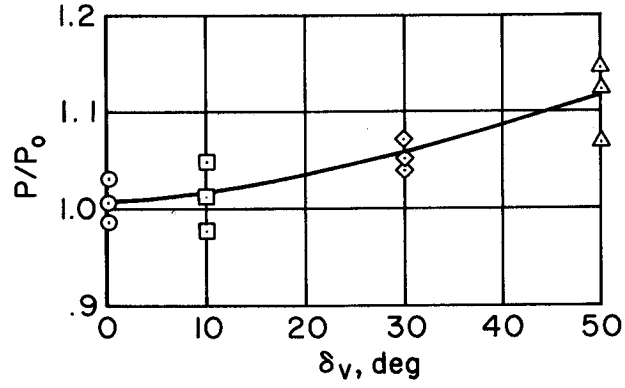

(c) Effect of vane deflection on power.

Figure 6.- Aerodynamic characteristics of the ducted fan with the 0° cascade with a vane chord-to-gap ratio of 0.83 at zero free-stream velocity; $\alpha = 0^\circ$.

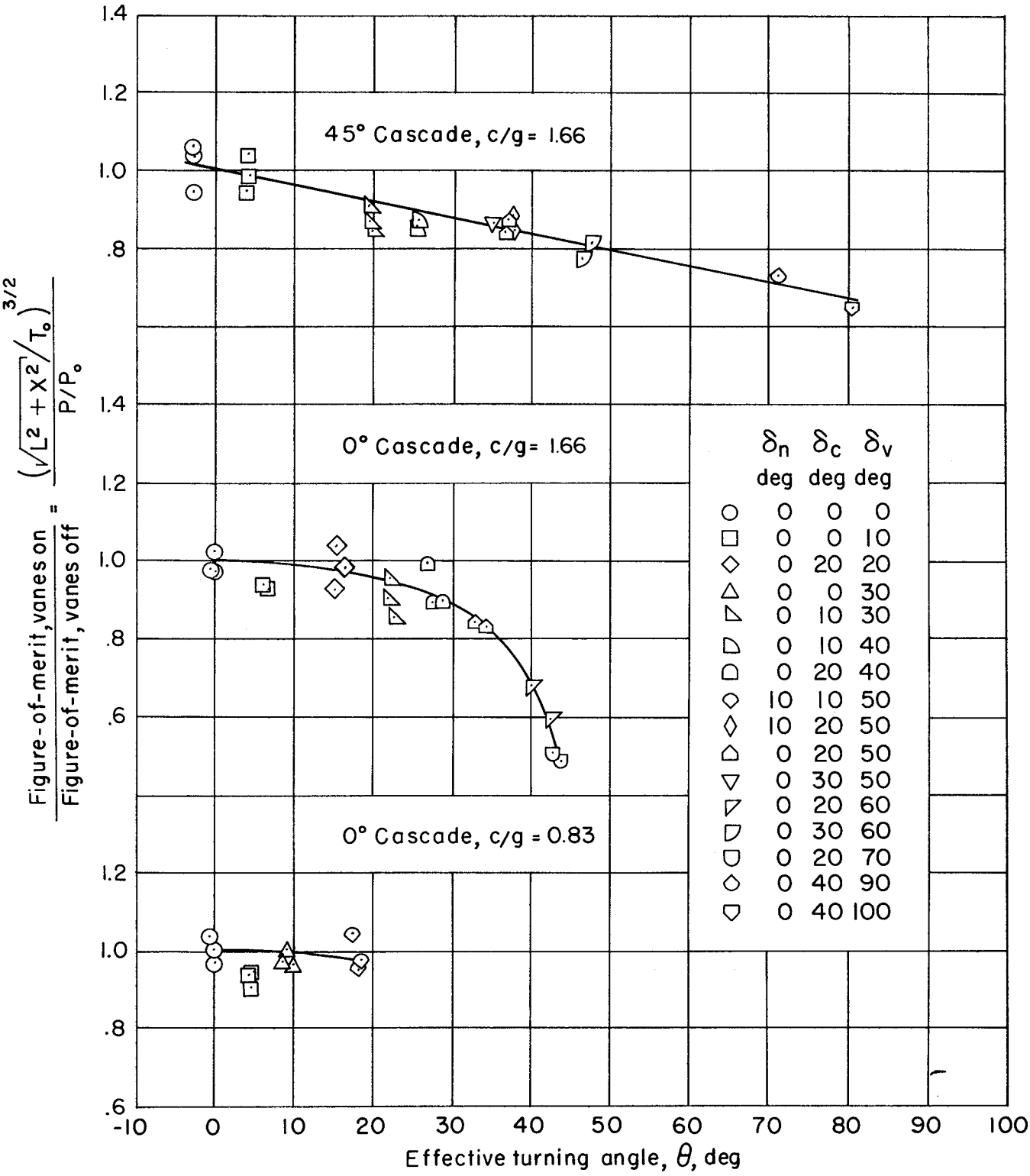

Figure 7.- Figure-of-merit ratio as a function of effective turning angle for $V_\infty = 0$.

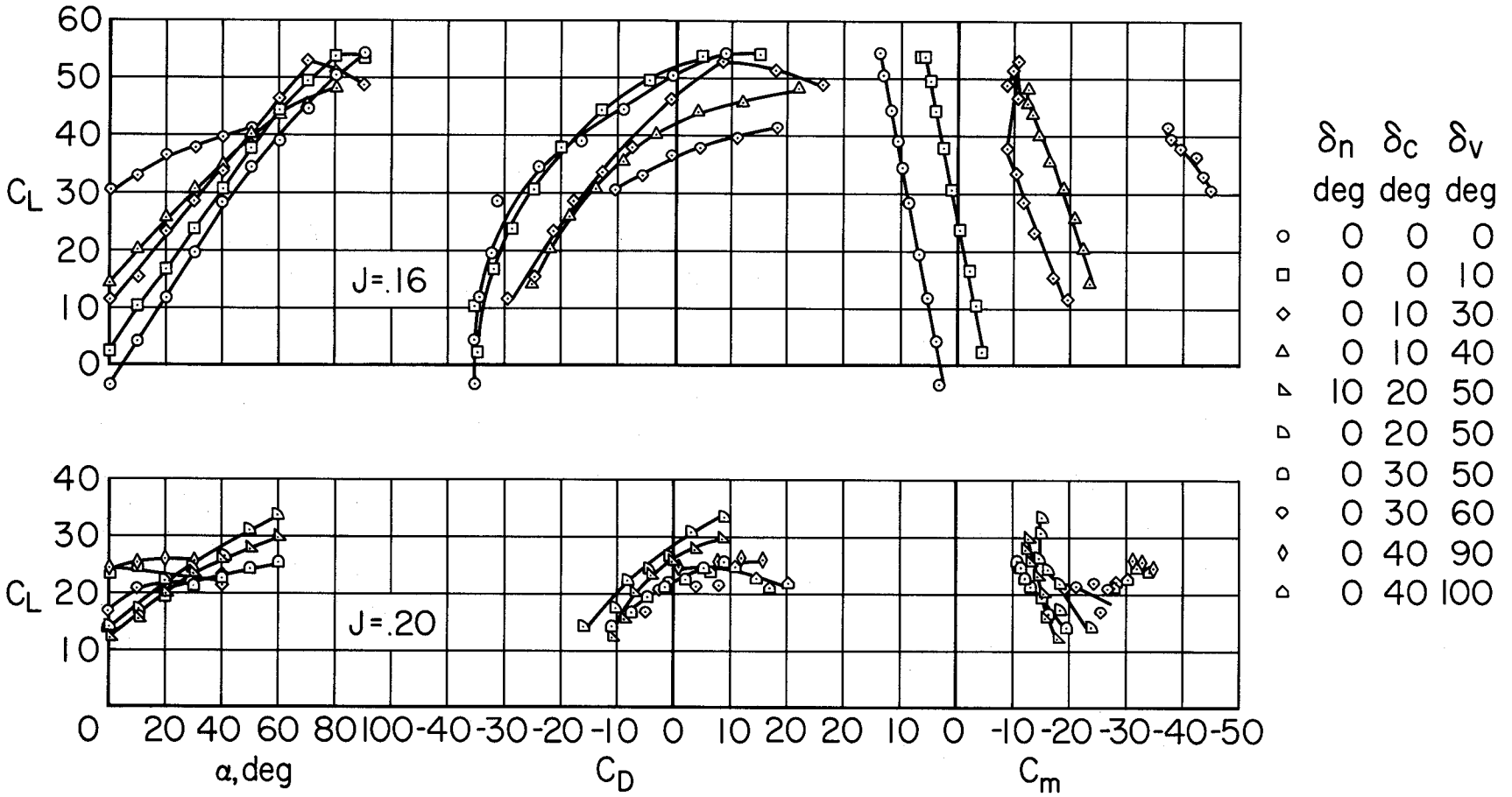

(a) J = 0.16, 0.20

Figure 8.- Aerodynamic characteristics of the ducted fan with the 45° cascade with a vane chord-to-gap ratio of 1.66.

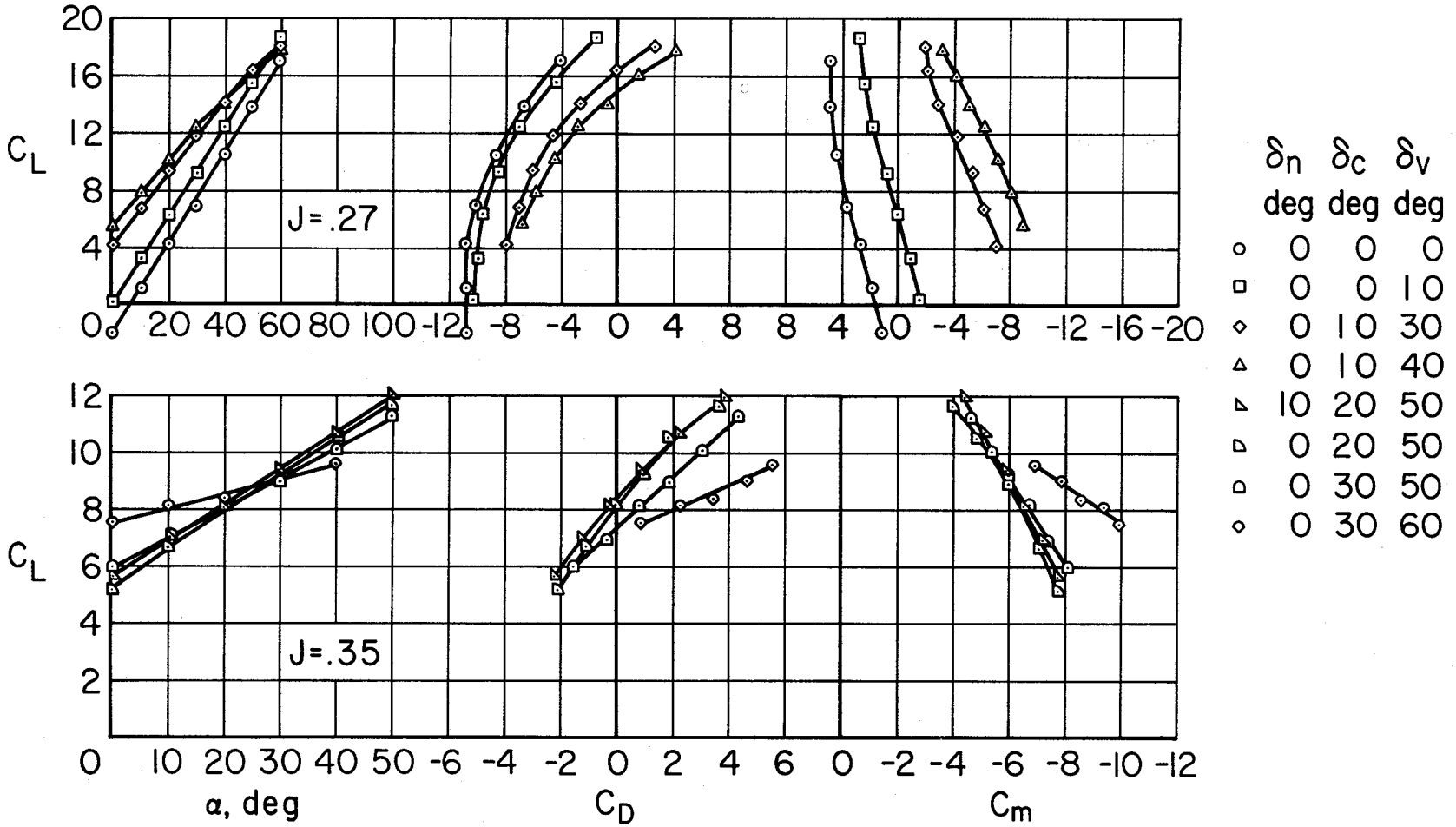

(b) J = 0.27, 0.35

Figure 8.- Continued.

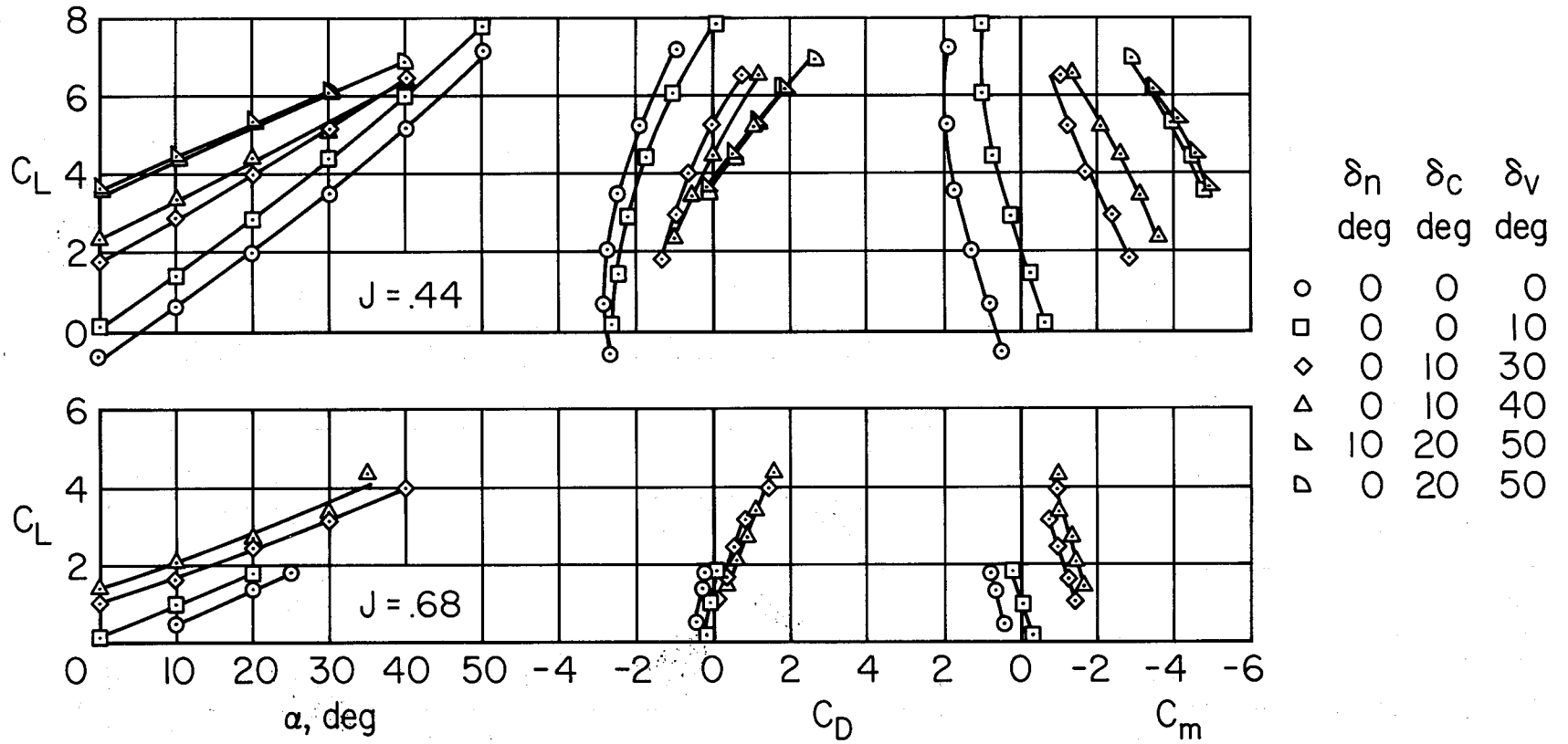

(c) J = 0.44, 0.68

Figure 8.- Concluded.

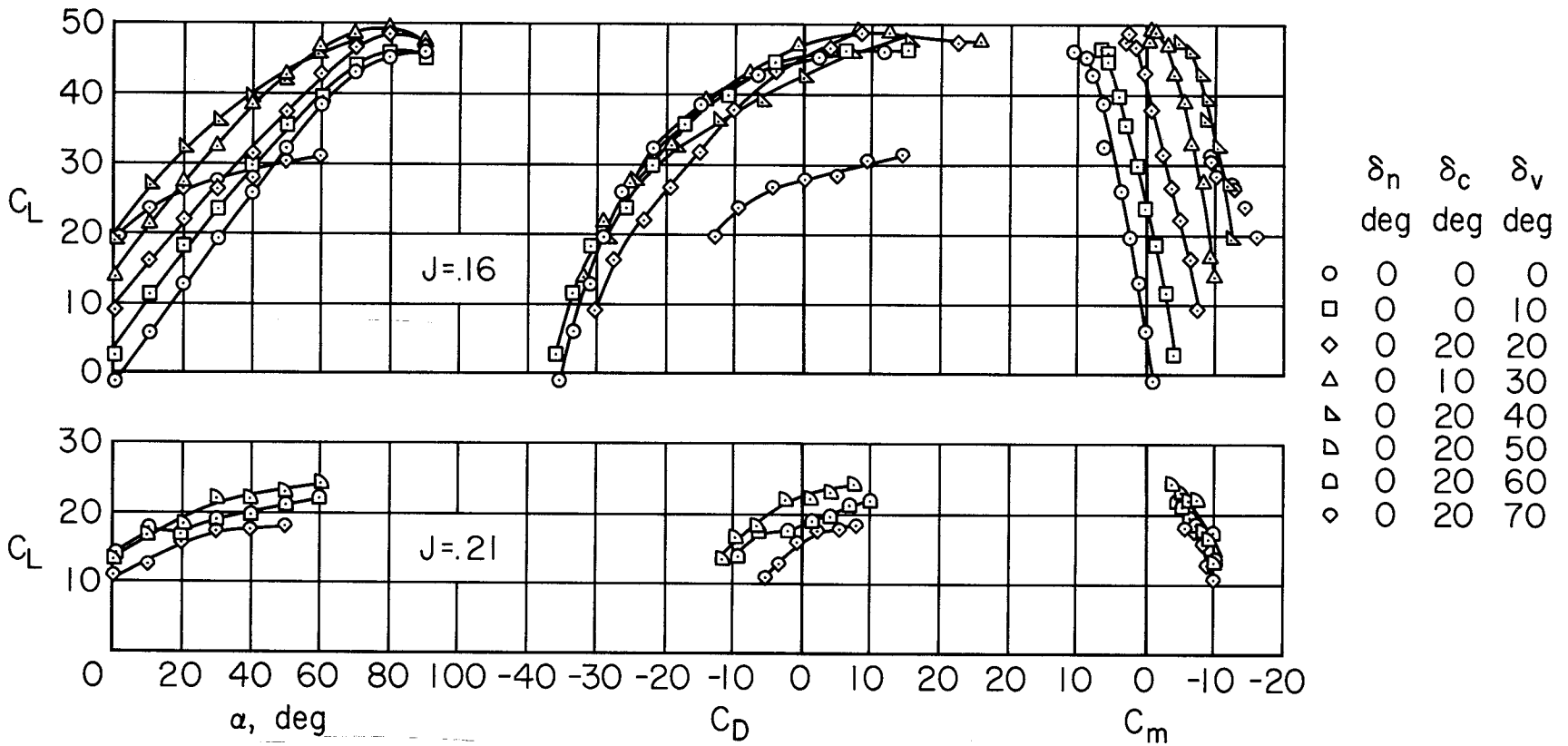

(a) J = 0.16, 0.21

Figure 9.- Aerodynamic characteristics of the ducted fan with 0° cascade with a vane chord-to-gap ratio of 1.66.

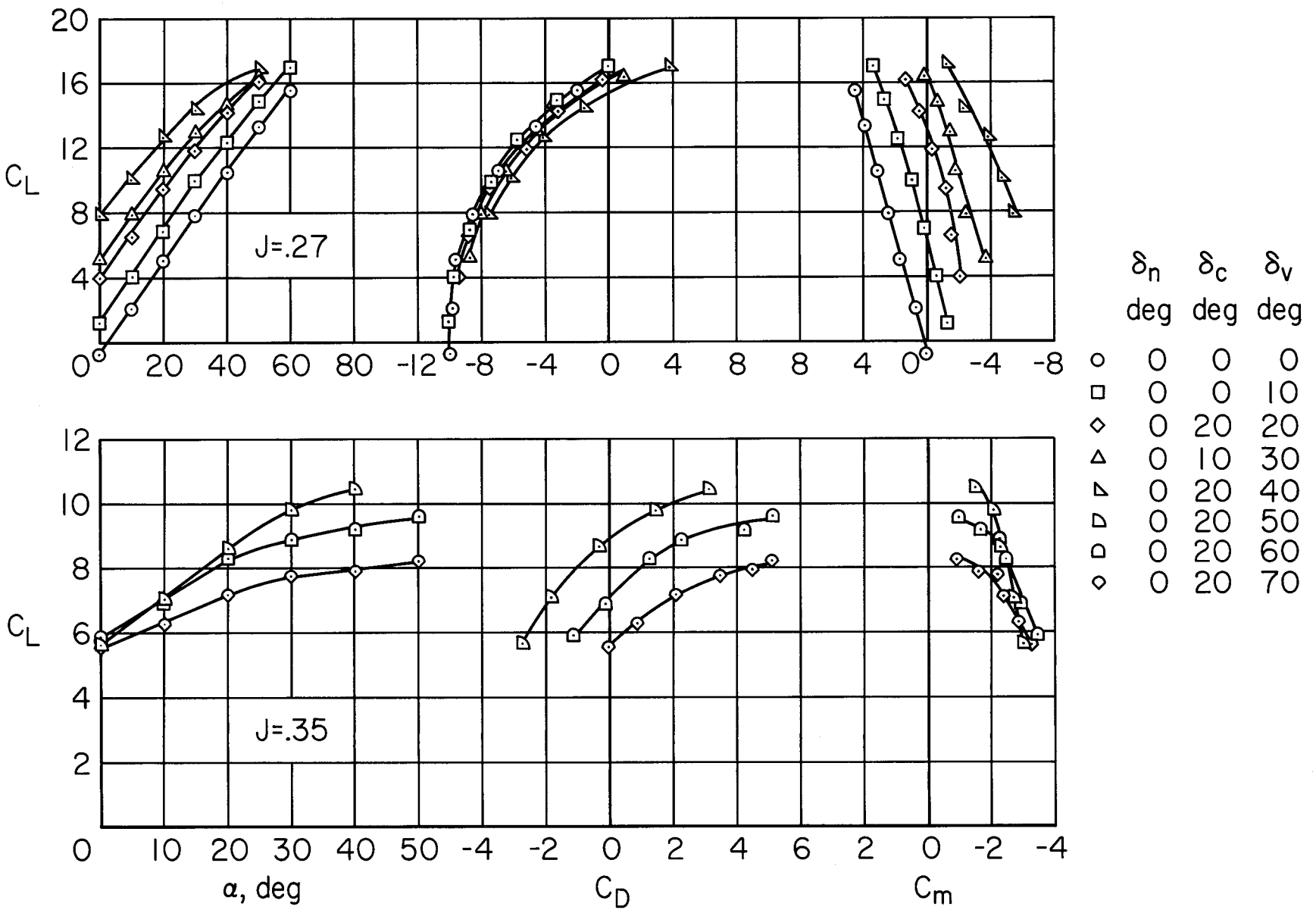

(b) J = 0.27, 0.35

Figure 9.- Continued.

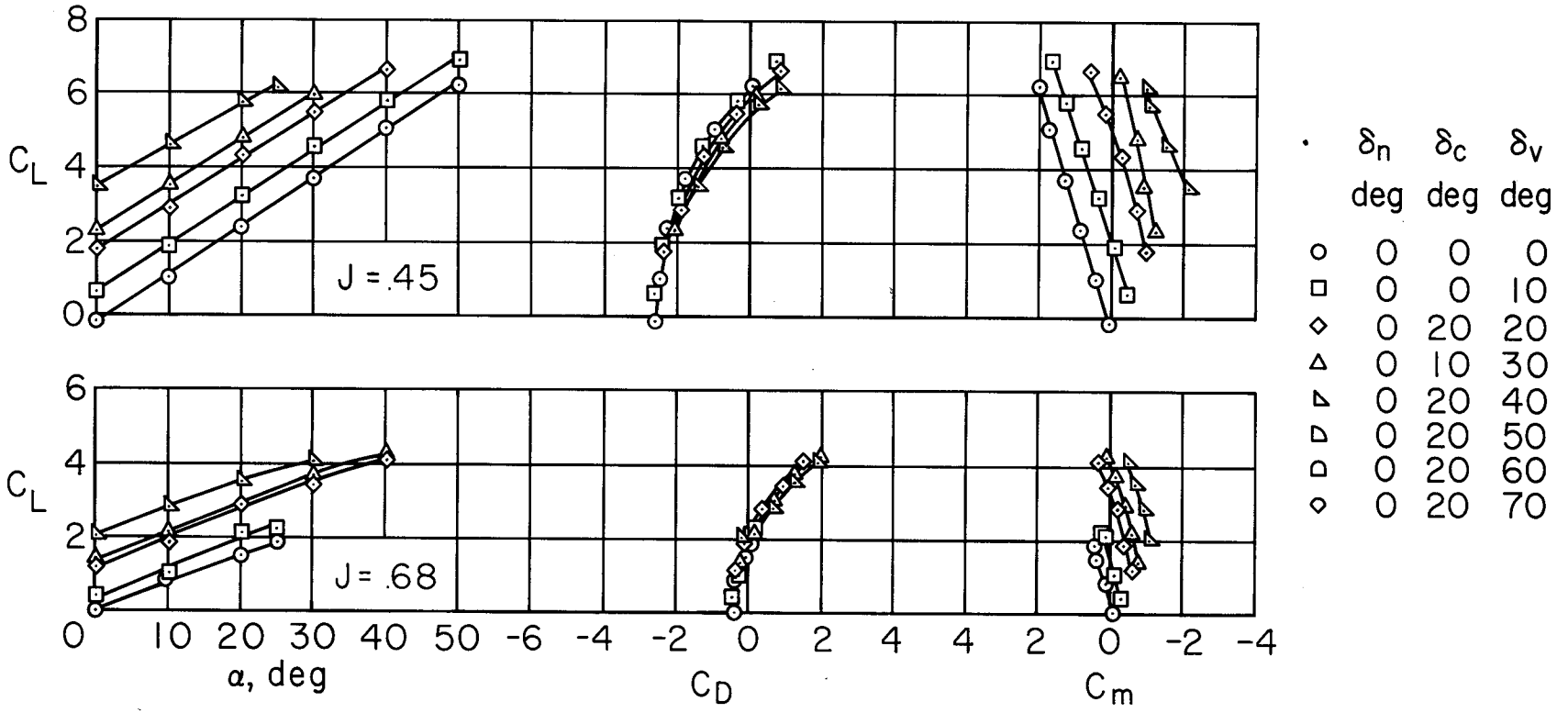

(c) J = 0.45, 0.68

Figure 9.- Concluded.

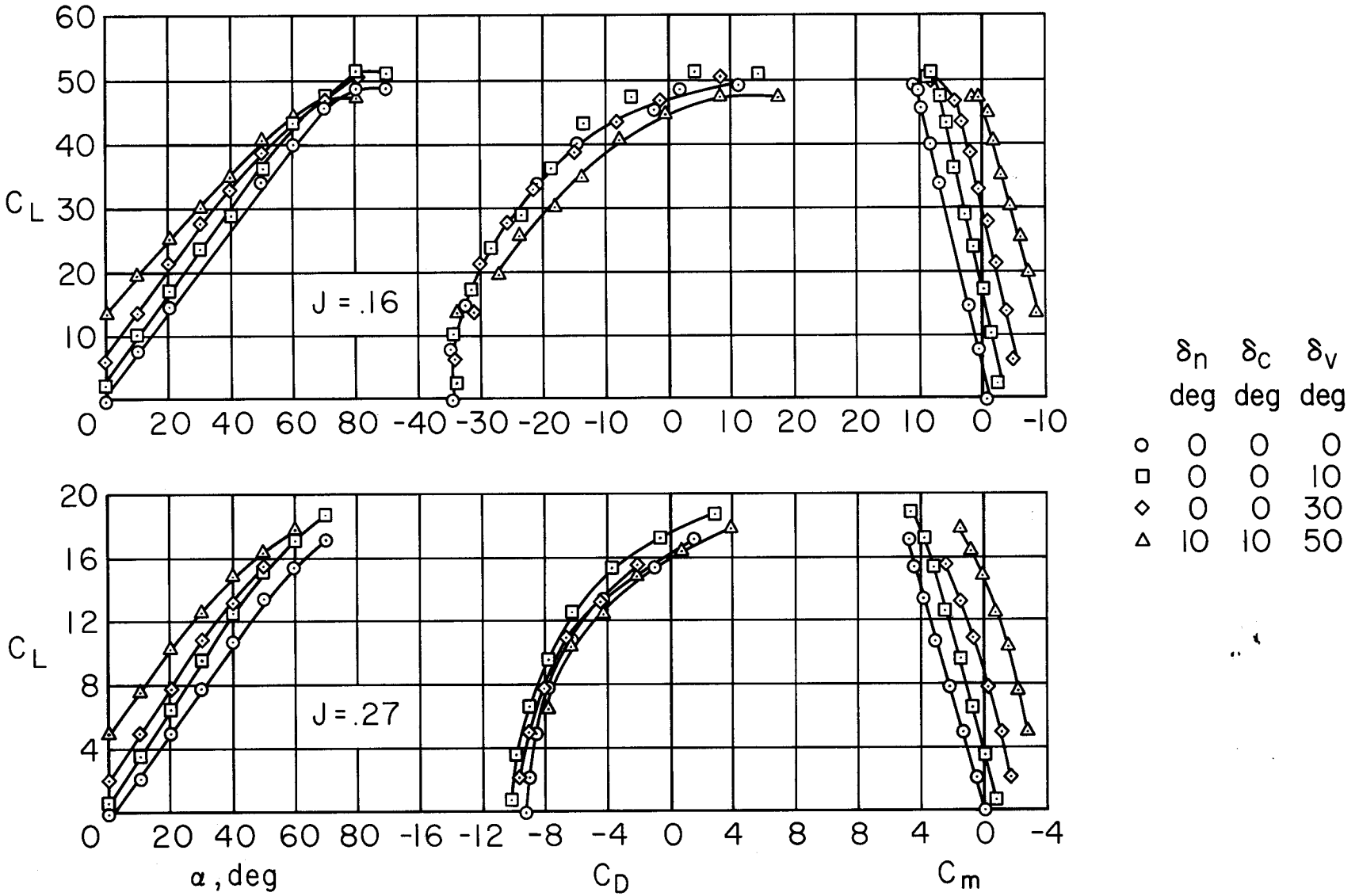

(a) J = 0.16, 0.27

Figure 10.- Aerodynamic characteristics of the ducted fan with 0° cascade with a vane chord-to-gap ratio of 0.83.

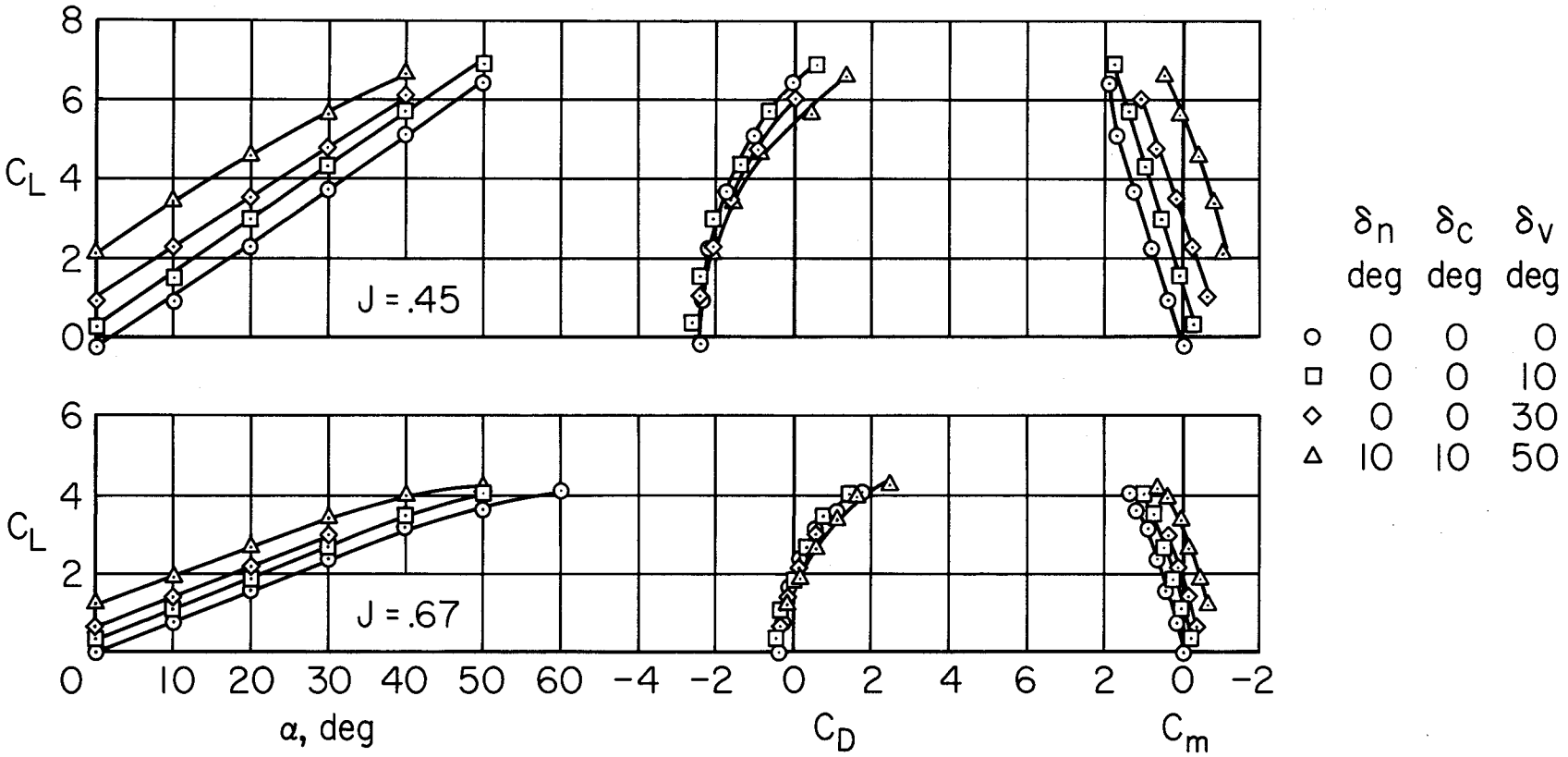

(b) J = 0.45, 0.67

Figure 10.- Concluded.

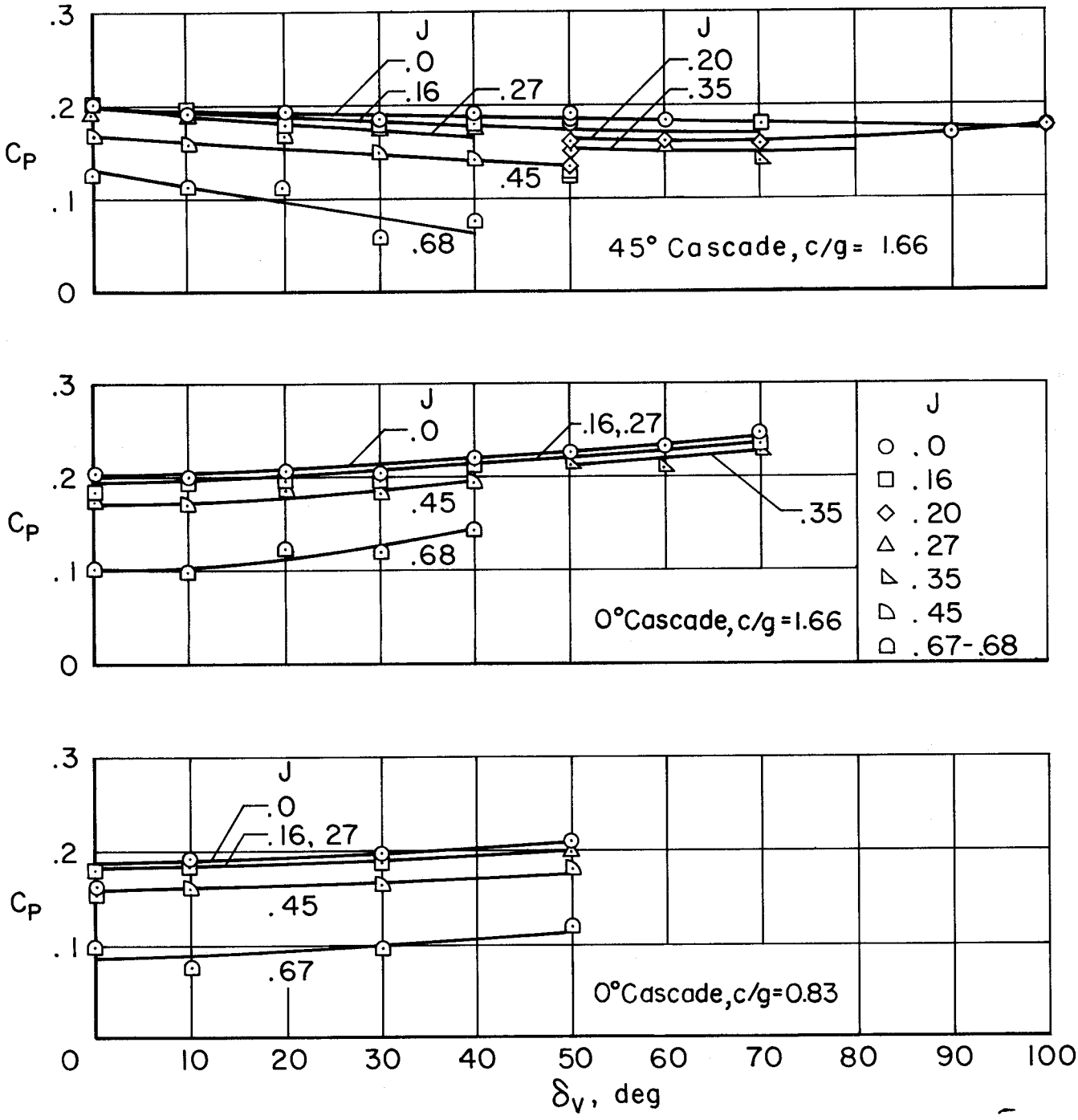

Figure 11.- Power coefficient as a function of vane deflection for the three vane configurations; $\alpha = 0^{\circ}$.

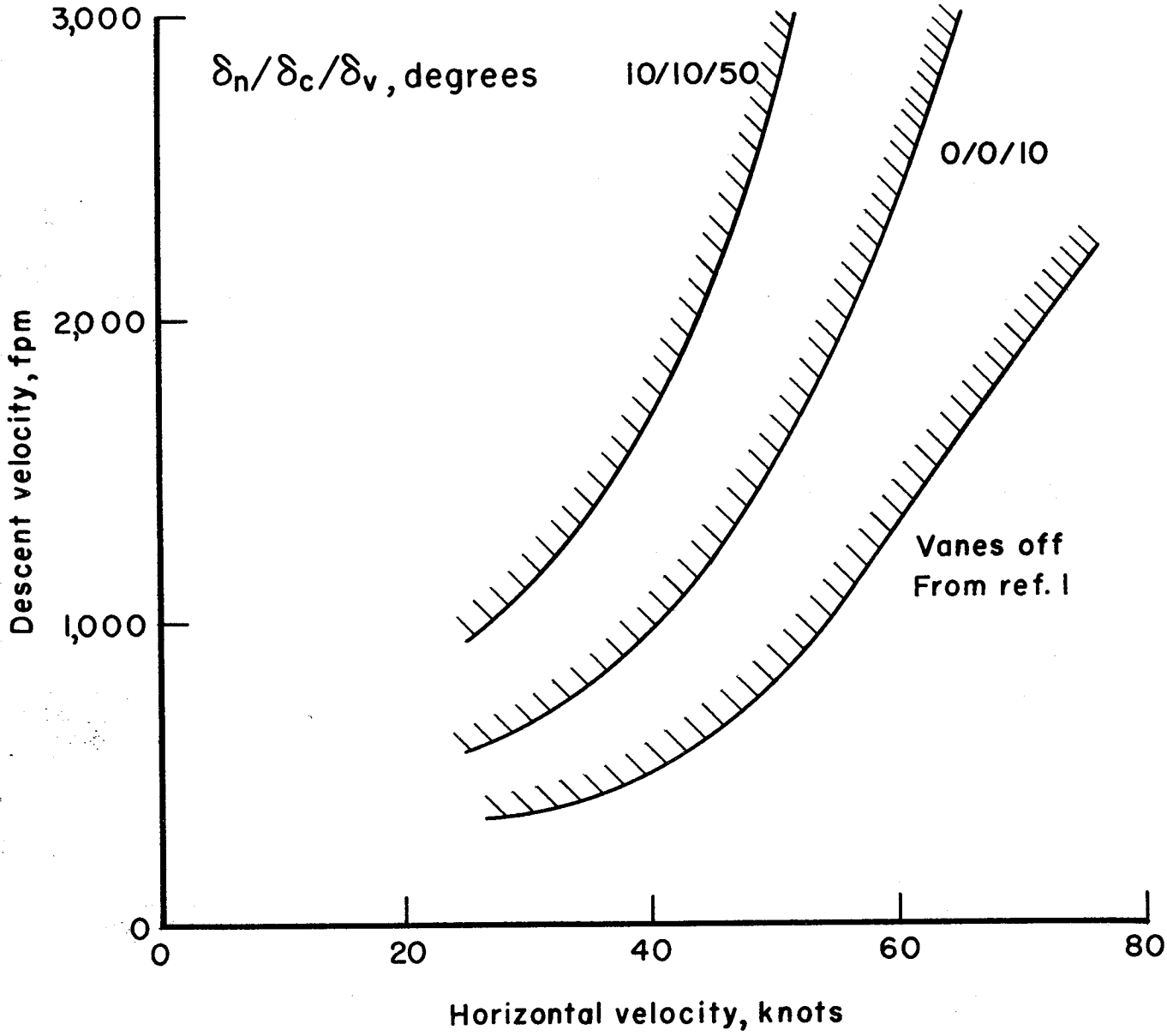

Figure 12.- Descent velocity boundary due to stall of the upstream duct lip for the vehicle of reference 1 at 0° wing angle of attack using the 0° cascade with a vane chord-to-gap ratio of 0.83.

NASA-Langley, 1964 A-822